Analysis of Fault-Induced Delayed Voltage Recovery Using EMTP Simulations

Krishnanjan Gubba Ravikumar and Scott Manson
Schweitzer Engineering Laboratories, Inc.

John Undrill
Private Contractor

Joseph H. Eto
Lawrence Berkeley National Laboratory

This paper was presented at the 2016 IEEE PES Transmission and Distribution Conference and Exposition, Dallas, Texas, May 2–5, 2016, and can be accessed at: http://dx.doi.org/10.1109/TDC.2016.7519960.

Analysis of Fault-Induced Delayed Voltage Recovery Using EMTP Simulations

Krishnanjan Gubba Ravikumar
Scott Manson
Schweitzer Engineering Laboratories, Inc.
Pullman, WA, USA

John Undrill
Private Contractor
Sedona, AZ, USA

Joseph H. Eto
Lawrence Berkeley National Laboratory
Berkeley, CA, USA

***Abstract*—This paper focuses on testing the dynamic behavior of single-phase air conditioner motors on distribution power networks. The primary goal is to study the phenomenon of delayed voltage recovery by applying multiple instances of a custom-built single-phase induction motor model on a given distribution feeder. This model was developed in an Electromagnetic Transients Program (EMTP) simulation environment. The motors were subjected to voltage disturbances seen in feeders experiencing the fault-induced delayed voltage recovery (FIDVR) phenomenon. To study the FIDVR phenomenon, a range of voltage depressions were simulated for predetermined system conditions. This paper describes a point-on-wave model development and simulation study that supports a broader investigation of the effect of air conditioning and similar loads on the recovery of electric utility voltage after faults.**

***Index Terms*—Air conditioner motor, delayed voltage recovery, Electromagnetic Transients Program (EMTP), fault-induced delayed voltage recovery (FIDVR), point-on-wave model.**

I. Introduction

Induction motors are predominantly used in households for air conditioning, refrigeration, and other purposes. These motors are believed to be the cause of the delayed voltage recovery seen in utility distribution systems in some parts of the United States [1] [2] [3] [4]. The phenomenon of slow recovery (in the order of seconds) of utility voltages after a fault is referred to as fault-induced delayed voltage recovery (FIDVR) [5].

A. Delayed Voltage Recovery

In an FIDVR event, the voltages in the subtransmission and distribution parts of a power system do not recover promptly to pre-event levels when the cause of a depression of voltages (normally an electrical fault) is removed.

A typical system configuration of concern is shown in Figure 1. A fault at a location such as Fault Location A in Figure 1 depresses voltages throughout the load area downstream of the fault location. Because the fault is external to the protection of the loads, clearing the external fault does not disturb the continuity of power to the loads. The expectation is that load voltages will return to normal values quickly when the fault is cleared. Typically, voltage recovers close to nominal following fault clearing; however, in FIDVR events, voltages in the load area do not recover promptly when the fault is cleared. Rather, the immediate increase in voltage when the fault is cleared is smaller than expected, and a full recovery to normal voltage takes many seconds [4]. A representative variation of voltage over a period of 120 seconds is shown in Figure 2.

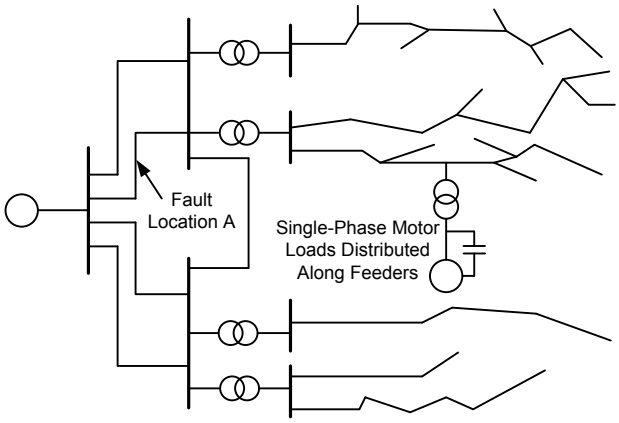

Figure 1. Typical System Configuration

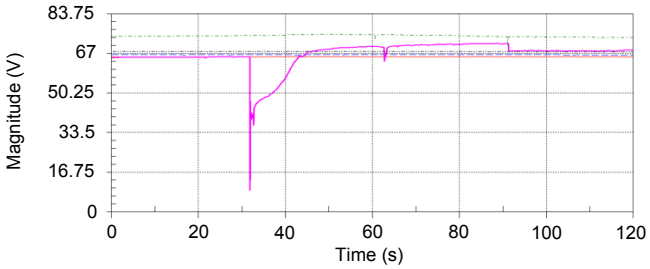

Figure 2. Representative Variation of Voltage Over a Period of 120 Seconds

B. Testing of Air Conditioners

The present understanding of the FIDVR phenomenon is that an initiating fault depresses voltages at the terminals of motors to such a degree that they stall. The inertia constants of small motors, particularly those driving residential air conditioner compressors, are very small (typically less than

40 milliseconds) and the run down to stall is correspondingly quick. Faults cleared in as little as 3 cycles have caused widespread stalling.

The present understanding of the phenomenon is largely based on the testing of individual air conditioners. Tests by Bonneville Power Administration (BPA) and Southern California Edison (SCE) have provided information on the behavior of individual motors when the amplitude of the voltage at the terminals is varied in sudden step changes, timed ramps, and oscillations in the electromechanical frequency band [6]. This testing gives a good indication of the voltage levels at which typical motors stall, both when voltage is reduced suddenly and when it is ramped at a moderate rate. Sudden-step testing is performed by reducing the applied voltage instantaneously to a given load. This testing has indicated that whether a motor stalls when the applied voltage is reduced suddenly to a given level is dependent on the phase of the voltage at the instant that the step is applied.

The testing by BPA and SCE was done with the air conditioners in normally loaded conditions, that is, with single-phase motors driving normal mechanical loads. This testing has not involved the measurement of the driven load itself.

C. Motor Simulation

A simulation model was developed by the authors to represent the behavior of a single motor and its driven load when subjected to variations of the applied terminal voltage. The model represents the electric motor at the level of electromagnetic transient simulations. Voltage, current, and flux variables are at the point-on-wave level, and the inductances of the machine vary sinusoidally with rotor angle. Mathematical rotational translations (e.g., Park's transformations) that would replace the sinusoidally varying inductances with constant values are not used. The simulation time step associated with the model is on the scale of 20 microseconds.

Electric machine models based on rotational transformations (Park's equations) cannot readily reproduce the presence or effects of unidirectional currents in the stator and rotor circuits. For example, these unidirectional currents are commonly seen as decaying dc currents and fluxes. The model used by the authors explicitly determines the flux in an electromagnetic transient form. This method has been proven to reproduce the effects of the dc currents and fluxes correctly. As expected, the model used by the authors is sensitive to the phase at which the applied voltage changes, while models based on rotational transformations cannot readily detect this phase effect. In short, the model used by the authors accurately depicts the field characteristics identified by BPA and SCE.

The same variations of terminal voltage used in the BPA testing were used in the model, and the resulting behavior of the currents and voltages was compared with test recordings. The absence of test recordings of load torque made it necessary for the simulation to use assumptions regarding load torque. Based on guidance from the Air-Conditioning, Heating, and Refrigeration Institute (AHRI), the load torque was assumed to consist of the following:

- A component proportional to the square of the speed, principally friction and windage load (T_{load}).
- A component varying with the angular position of the crankshaft of the driven reciprocating or scroll compressor (T_{av}).

To represent the suggested AHRI characteristics, the load torque used by the authors is illustrated in Figure 3. This is a triangular waveform with a dc offset.

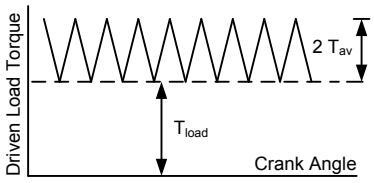

Figure 3. Load Torque Profile Used in Simulations

The simulation with one single-phase motor corresponded well to the test results obtained previously from a different modeling environment. It corresponded well with regard to the voltage levels at which the motor stalled and with regard to the dependence of a stall on the phase of the applied voltage at the moment the voltage was reduced.

II. Elements of the Simulation

One objective of the simulation was to apply the validated single-phase motor and load model on a distribution feeder or subtransmission system. To do this, a distribution feeder model was built with a load consisting mostly of small single-phase motors.

A. Single-Phase Motor Model

The single-phase motor model is a first-order forward difference implementation of an electromagnetic model of a single-phase induction motor and its associated capacitor (this model represents a permanent split-capacitor ac induction motor) [7]. Figure 4 shows the placement of the stator and rotor windings, where Θ is the physical angular position of the rotor winding centerline relative to the stator structure, A and B are windings, and *x* is the pole of the machine.

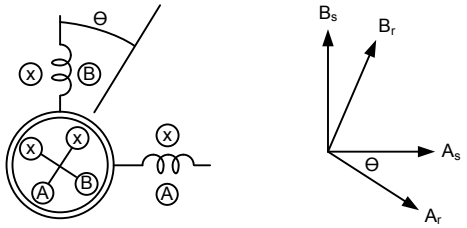

Figure 4. Induction Motor Model Recognizing Sinusoidal Variation of Mutual Inductances

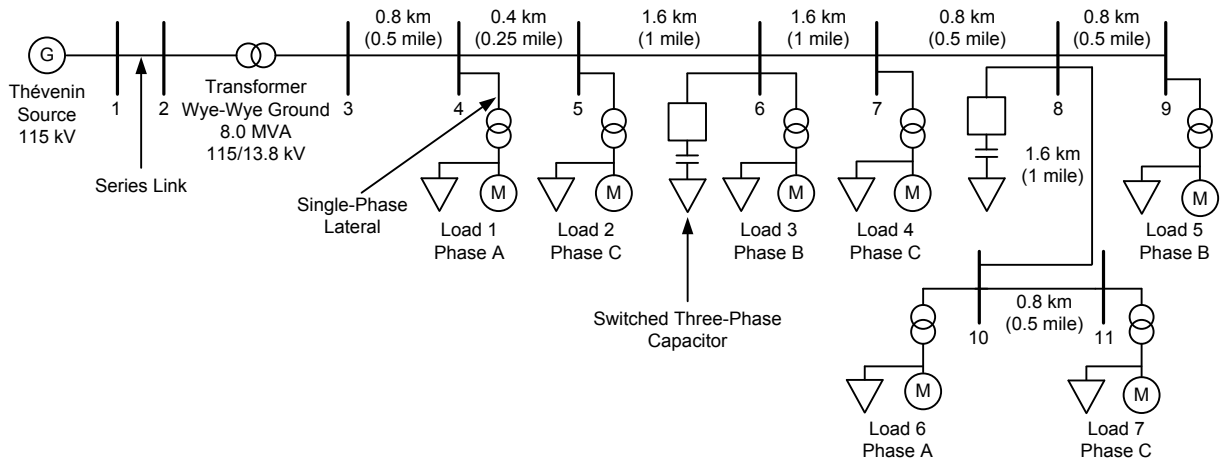

Figure 5. Feeder Layout Used for Simulations

B. Distribution Feeder and Transformer

The study considers the feeder shown in Figure 5. The distribution feeder model is made up of three-phase line sections with parameters specified in terms of symmetrical component impedances. The single-phase distribution transformers that connect the load to the feeder model are connected from phase to ground. Individual blocks of load are located on radial single-phase lateral lines, represented by simple series impedances. Each block of load is located at the end of a single-phase lateral and consists of a distribution transformer, a purely resistive load, and a single-phase 230 V air conditioner motor.

C. Power Supply and Applied Voltage Dips

The three-phase source in the 115 kV section of the system is operated at 121 kV (in a typical operating scenario). The voltage source is modeled by a strong 121 kV Thévenin source and a simple series impedance. The source is modeled as a three-phase programmable source, thus providing control over voltage magnitude, phase, and frequency for each phase. This source voltage is programmed to simulate subtransmission and transmission events.

D. Feeder Loading

The feeder is set up with strongly unbalanced loading. Phase C serves three loads, while Phases A and B serve two loads each. Phase C is very heavily loaded and has a greater than normal voltage drop from its head (transformer) to the last load at Bus 11 (see Figure 5).

E. Air Conditioner Loading

The simulations examine the behavior of the air conditioners at the loading levels shown in Table I.

TABLE I RANGE OF AIR CONDITIONER LOADING LEVELS

Nominal Power (kW)	Speed-Dependent Torque (Nm)	Triangular Torque (Nm)	Average Torque (Nm)
4.52	8	4	12
5.28	6	8	14
6.03	4	12	16

This range of power corresponds approximately to the range of power used by a 13.00 Seasonal Energy Efficiency Ratio-rated (SEER-rated) air conditioner under ambient temperatures. The triangular component of the load torque has two peaks per revolution of the motor and therefore corresponds to a two-cylinder compressor.

III. REAL-TIME SIMULATOR

A. Simulator Operation

The hardware-based Electromagnetic Transients Program (EMTP) simulator used for this paper is a fully digital power system simulator capable of continuous real-time operation. It performs electromagnetic power system transient simulations, with a typical simulation time step in the order of 50 ms, using a combination of custom software and hardware.

For this project, the real-time EMTP simulator was specifically used to study the behavior of multiple single-phase induction motors in point-on-wave detail when connected to a distribution feeder model.

Because the single-phase induction motor was custom built in the simulator, it had to be externally interfaced to the simulator network solution.

B. Initialization and Sequence of Events

Each simulation was initialized by picking up the feeder, allowing the motors to run up to speed against minimal load, applying the driven loads, and allowing conditions to stabilize before applying a voltage dip. The sequence of events is shown in Table II.

TABLE II SEQUENCE OF EVENTS USED FOR ALL SIMULATIONS

Time (s)	Action Taken
0.0	Energize feeder (Van, Vbn, and Vcn = 70.0 kV L-N at source)
0.5	Apply driven loads
1.0 + phase delay	Apply programmed dip in source voltages

IV. Simulation Results

A. Motor Behavior in Steady Conditions

Because the windings of the motor have a different number of turns and carry different currents, the torque developed by the motor contains a significant component varying at twice the supply frequency. The load torque contains the triangular component associated with the crank angle, which varies at a frequency of twice the rotor speed. The average rotor speed is slower than the synchronous speed. The instantaneous rotor speed is not constant but varies in accordance with the variation of electromagnetic and load torques. The waveform of the driven load torque is synchronous with the rotor angle; therefore, it is not synchronous with the waveform of electromagnetic torque.

The result of the nonsynchronism of the driving and resisting torques is that the variation of rotor speed is not constant, even in steady supply conditions. Instead, the variations of electromagnetic torque, load torque, and rotor speed all follow a beat frequency pattern determined by the difference between the synchronous and rotor speeds. Because the waveform of rotor-synchronized load torque slips in phase constantly with respect to the phase of the supply voltage, the internal condition of the motor at the moment of inception of a disturbance is a function of the operational history of the driven load.

Figure 6 illustrates the slipping of the load torque waveform with respect to the double frequency variation of the electromagnetic torque.

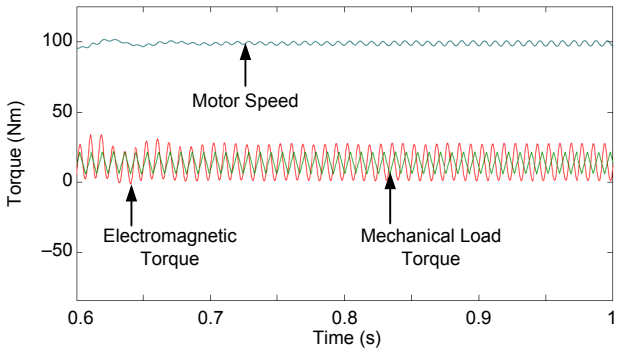

Figure 6. Slipping of Load Torque With Regard to Electromagnetic Torque During Steady-State Stalling Mechanism

The load torque variation is substantially in phase with the electromagnetic torque at 0.6 seconds and in complete phase opposition at 0.95 seconds. It is evident that simulations applying voltage dips at different times (at 1.5 seconds rather than at 1 second, for example) would be expected to provide slightly different results.

B. Mechanism of Stalling

When the motor terminal voltage is reduced suddenly, large but brief negative decelerating excursions of the electromagnetic torque are observed. These components of torque are associated with the unidirectional and low-frequency transient components of current that are induced in the inductive windings of the motors when voltages are changed quickly. In these simulations, where the amplitude of the supply voltage is changed suddenly, the nonsinusoidal transient components of current depend on the phase of the supply voltage at the instant of the change. Accordingly, the transient variation of electromagnetic torque is strongly dependent on the phasing of the applied voltage dip. Then, as noted in the previous subsection, the relative phase of the supply voltage and the load torque are highly variable.

C. Summary of Simulation Results

Overall, 350 simulation runs were performed for different combinations of the preidentified stall-sensitive parameters. The parameters used for illustrating the sensitivity of motor stalling are shown in Table III.

Table III Stall-Sensitive Parameters

Voltage at Bottom of Dip, 70 kV Nominal (kV)	Voltage Dip (%)	Voltage Phase Angle During Dip Initiation	Voltage Dip Duration (cycles)	T_{load} (Nm)	T_{av} (Nm)
25.2	36	0°	3	8	4
30.5	43.5	30°	5	6	8
35.9	51.2	60°	7	4	12
41.2	58.8	90°	9	NA	NA
46.5	66.4	NA	NA	NA	NA

The simulation results were captured in the form of COMTRADE files and comma-separated value (CSV) tables. The COMTRADE files contained the power system dynamics information for every run, including plots of three-phase voltages and currents (i.e., instantaneous plots, root-mean-square [rms] plots per phase, and sequence quantities per phase), motor terminal voltages, motor speeds, and motor electromagnetic torques. The CSV tables contained flagging results for the motor stall condition for every run. Flags indicate which motors stalled and which did not.

The statistical results of motor stalls for some stall-sensitive parameters are shown in Figure 7. The following observations are evident from these simulations:

- The longer the fault duration, the higher the number of stalled motors.
- The larger the voltage dip, the higher the number of stalled motors.
- The higher the motor loading, the higher the chances for stalling. For example, with the average load torque of 12 Nm, the supply voltage must be severely depressed to cause motors to stall. However, at 14 Nm load torque, some motors stall when the voltage dips to only 66 percent of the pre-event level.

The entire simulation resulted in approximately 5 GB of plot data. Because it is not practical to present all of the simulation results in this paper, a discussion of the results is presented in the next section, along with some qualitative conclusions.

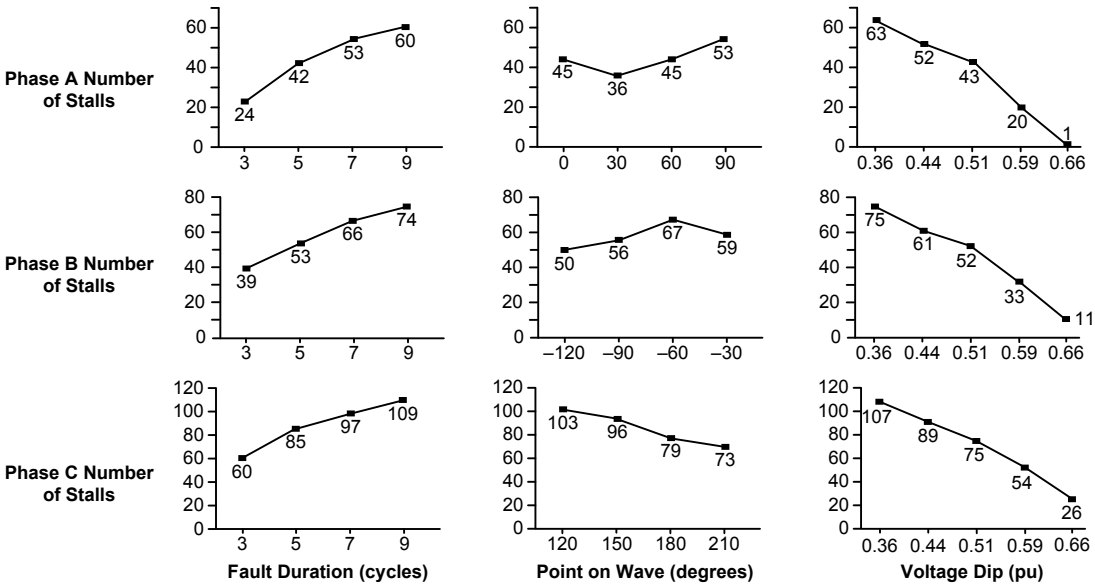

Figure 7. Statistical Stall Numbers Showing Sensitivity to Preidentified Parameters

V. Conclusion

It is necessary to represent both the electrical behavior of single-phase capacitor motors and the driven loads in point-on-wave detail to obtain a faithful simulation of the test behavior of residential air conditioners.

The numerical values of voltage, load torque, and duration of dip appearing in this study cannot be regarded as a useful guide as to whether motors on a real feeder will stall. However, they are useful as an indication of the relative effect of the many parameters that can affect motor stalling or reacceleration. The values support the following largely qualitative conclusions:

- The likelihood that motors will stall is strongly related to their loading. When the load is air conditioning, there is a strong correlation between stalling and high ambient temperature.
- Stalling of air conditioner motors does not require a long duration of voltage dip. With moderate loading, most or all motors will stall in a 9-cycle dip, and some will stall in a dip of only 3 cycles.
- It is quite credible that nearly all motors on a feeder will stall in a dip as brief as 3 cycles when their driven loads are near maximum.

The behavior of the motors indicated by a limited number of point-on-wave motor models connected to a very simplified distribution feeder model supports the conclusions indicated by working with a single instance of the model. Stalling depends on a wide range of factors and can occur quickly in relation to the time scale of bulk electric system disturbances.

This project supports the emerging deduction from field experience that stalling of air conditioner motors must be expected to occur not only following longer than normal electric system faults but also in the wake of normal and properly cleared disturbances.

The handling of motor behavior in simulations of the bulk electric system should have a basis in a statistical understanding of the prevalence of motor-stalling events. It is desirable to have a real-time simulator available for focused studies. In particular, it is desirable to obtain data from a well-instrumented feeder and to be able to simulate that feeder response to played-back recordings of events.

References

[1] G. L. Chinn, "Modeling Stalled Induction Motors," proceedings of the 2005/2006 IEEE PES Transmission and Distribution Conference and Exhibition, Dallas, TX, May 2006.

[2] B. R. Williams, W. R. Schmus, and D. C. Dawson, "Transmission Voltage Recovery Delayed by Stalled Air Conditioner Compressors," *IEEE Transactions on Power Systems*, Vol. 7, Issue 3, August 1992, pp. 1173–1181.

[3] J. W. Shaffer, "Air Conditioner Response to Transmission Faults," *IEEE Transactions on Power Systems*, Vol. 12, Issue 2, May 1997, pp. 614–621.

[4] "NERC Technical Reference Paper on Fault-Induced Delayed Voltage Recovery, Version 1.2" NERC Transmission Issues Subcommittee and System Protection and Control Subcommittee, June 2009. Available: http://www.nerc.com.

[5] B. Lesieutre, R. Bravo, R. Yinger, D. Chassin, H. Huang, N. Lu, I. Hiskens, and G. Venkataramanan, "Load Modeling Transmission Research: Appendix D – Recommended Model for Single Phase Compressor," March 2010. Available: http://web.eecs.umich.edu/~hiskens/ publications/LM_Final_Report.pdf.

[6] B. Lesieutre, D. N. Kosterev, and J. Undrill, "Phasor Modeling Approach for Single Phase A/C Motors," proceedings of the 2008 IEEE Power and Energy Society General Meeting, Pittsburgh, PA, July 2008.

[7] Y. Liu, V. Vittal, J. Undrill, and J. H. Eto, "Transient Model of Air-Conditioner Compressor Single Phase Induction Motor," *IEEE Transactions on Power Systems*, Vol. 28, Issue 4, November 2013, pp. 4528–4536.

Previously presented at the 2016 IEEE PES Transmission and Distribution Conference and Exposition, Dallas, TX, May 2016.

20150805 • TP6611